Journal of NeuroVirology, 12: 420–427, 2006

ISSN: 1355-0284 print / 1538-2443 online
DOI: 10.1080/13550280601009546

informa
healthcare

ICP47 mediates viral neuroinvasiveness by induction of TAP protein following intravenous inoculation of herpes simplex virus type 1 in mice

Javier S Burgos, Esther Serrano-Saiz, Isabel Sastre, and Fernando Valdivieso

Departamento de Biología Molecular and Centro de Biología Molecular Severo Ochoa (C.S.I.C.-U.A.M.), Universidad Autónoma de Madrid, Madrid, Spain

Herpes simplex virus type 1 (HSV-1) expresses an immediate-early protein, ICP47, that blocks the major histocompatibility complex class I antigen presentation pathway by binding to the transporter associated with antigen presentation (TAP). The result is the virus' evasion of the immune system. Although the interaction between ICP47 and TAP has been examined *in vitro*, this paper is the first to report their interaction *in vivo*. In C57BL/6 adult female mice, ICP47-defective virus (ΔICP47, F strain) was less able to invade the organs studied than was wild-type HSV-1 F strain, showing that ICP47 influences general invasiveness. However, the neuroinvasiveness of the ΔICP47 virus was recovered in TAP-deficient mice, indicating that the TAP-ICP47 interaction is specific to neural tissues. HSV-1 F strain showed no significant differences in their invasiveness in TAP-deficient and wild-type mice. Therefore, although ICP47 appears to be essential for invasion, the presence of TAP appears not to be crucial. Western blotting showed TAP1 expression to increase by at least fourfold in the brains and adrenal glands of infected mice. This suggests that TAP plays an important role in the host defense system. This increased expression may be particularly important in the encephalon since the baseline protein levels of this organ are low (ratio adrenal protein level/encephalon protein level > 100). However, ΔICP47 virus provoked no significant increase in the brain TAP1 levels of wild-type mice because it could not invade this organ. These results suggest that ICP47 plays a role in infection, and that TAP1 production is regulated during viral challenge. *Journal of NeuroVirology* (2006) **12,** 420–427.

Keywords: brain; herpes simplex virus type 1; ICP47; mice; TAP

Introduction

Evading the immune system is vital to the survival of persistent viruses such as herpesviruses. These establish latent infections often lasting the lifetime of an infected individual. The recognition of virus-infected cells by T lymphocytes is strongly dependent on the presentation of antigenic fragments derived from viral proteins, bound to the major histocompatibility complex (MHC) class I molecules (Townsend and Bodmer, 1989). In an attempt to remain undetected, herpesviruses interfere with antigen presentation (Hill and Ploegh, 1995). In fact, in human fibroblasts, herpes simplex virus (HSV) infection causes the rapid inhibition of MHC class I antigen presentation, leading to the accumulation of class I heavy chain and β_2-microglobulin (HC-β_2-m) complexes in a peptide-empty form in the endoplasmic reticulum (ER) (Hill *et al*, 1994; York *et al*, 1994). The immediate-early protein ICP47 (IE12), coded for by the HSV type 1 (HSV-1)

Address correspondence to Javier S. Burgos or Prof. Fernando Valdivieso, Lab. CX340, Centro de Biología Molecular, Universidad Autónoma de Madrid, 28049 Cantoblanco, Madrid, Spain. E-mail: jburgos@cbm.uam.es; fvaldivieso@cbm.uam.es

J.S.B. and E.S.-S. contributed equally to this work.

This work was supported by a grant from the Obra Social Caja Madrid to the Asociación de Familiares de Enfermos de Alzheimer (AFAL), and by an institutional grant by the Fundación Areces to the Centro de Biología Molecular Severo Ochoa. The authors thank Prof. F. Mayor for continuous encouragement and help, and Dr. B. Roizman for providing the HSV-1 F strain mutant.

Received 6 July 2006; revised 19 August 2006; accepted 7 September 2006.

genome, plays an important role in this (York *et al*, 1994).

The transporter associated with antigen processing (TAP) (Spies *et al*, 1990) (a heterodimer composed of two proteins, TAP1 and TAP2) plays a critical role in the MHC class I antigen processing pathway by transporting viral antigenic peptides from the cytosol to the ER. Upon reaching the plasma membrane they are presented on the cell surface where they are recognized by $CD8^+$ T cells. Inheritable TAP deficiency in humans (type 1 bare lymphocyte syndrome) is manifested as a down-regulation of MHC class I molecules (Gadola *et al*, 2000); clinically it is responsible for recurrent infections and narcotizing skin lesions in early life.

In the present study, TAP-deficient mice were used to as a model of human TAP deficiency. ICP47 dramatically inhibits peptide translocation in permeabilized mammalian cells (Fruh *et al*, 1995; Hill *et al*, 1995) via its union with the peptide binding site of TAP, where the core sequence of the ICP47 for TAP inhibition has been mapped (Galocha *et al*, 1997). This prevents TAP binding with other suitable substrates (Ahn *et al*, 1996; Tomazin *et al*, 1996). An animal model that reflects the effects of ICP47 on human TAP deficiency is therefore highly desirable. At first sight it might appear that a mouse model is inappropriate because ICP47 inhibits murine TAP relatively poorly (Ahn *et al*, 1996; Fruh *et al*, 1995; Hill *et al*, 1995; Orr *et al*, 2005; Tomazin *et al*, 1996; York *et al*, 1994). However, Goldsmith *et al* (1998) successfully used a murine ocular model to investigate HSV-1 ΔICP47 infection (in comparison with a rescue virus). To date, this is the only work to report differences in neuroinvasiveness associated with ICP47, but its scope was restricted to the neural route of infection (corneal scarring). No other routes were explored and the role of TAP was not analyzed. However, this study was restricted to BALB/c female mice that are very susceptible compared to C57BL/6 mice. A number of factors as the mouse strain, the inoculation route, or the viral dose may vary in susceptibility to infection with herpesviruses.

Infection of HSV-1 usually occurs via the oral, ocular, or genital routes (Johnson, 1964) and possibly occurs via the hematogenous route. The latter, however, is the main route by which immunosuppressed individuals and neonates are infected (Arvin *et al*, 1982; Montgomerie *et al*, 1969). Although the main route for HSV-1 infection is certainly neural, hematogenous infection could be important in some contexts. In fact, inoculation into the bloodstream has been used consistently in animal models for the study of HSV-1 pathogenesis, and, to that effect, our group has described that, in mice, the bloodstream is the natural route by which the progeny of latently infected mothers are challenged (Burgos *et al*, 2006b). Hematogenous infection is also well known to occur in young (Johnson, 1964; Kern *et al*, 1973; Lascano and Berria, 1980) and adult animals (Burgos *et al*, 2002a, 2003, 2005). Although the neurovirulence depending on ICP47 viral protein has been analyzed in a neural context (Goldsmith *et al*, 1998), the role of ICP47 and its relationship with murine TAP *in vivo* have never been examined in bloodstream-infected animals.

The aim of this work was to determine the role of ICP47 and its relationship with TAP in mice hematogenously infected with HSV-1. Particular attention was paid to the importance of this relationship in the infection of the nervous system.

Results

Clinical scores

After inoculation with several doses of 10^6, 10^7, or 10^8 plaque forming units (PFU) of virus (F strain or ΔICP47), none of the mice showed any clinical symptoms of disease. None of the mock-infected animals showed any clinical abnormalities.

Infection time course

The number of viral genomes per host DNA showed the blood to have a constant viral DNA level until 10 days post inoculation (dpi) (Figure 1). During the initial stages of the infection, HSV-1 F strain DNA was detected in the mesenteric lymph nodes, but was cleared after day 5.7. The ovaries showed a peak of infection at day 2, after which viral DNA levels decreased ($P < .05$). Levels in the adrenal glands increased from the time of first detection (day 0.8) until day 4 when viral DNA appeared in the spinal cord. On day 4, viral DNA was also detectable in the brain (coinciding with the clearance in the spinal cord and indicating the order of neuroinvasion), increasing in concentration until day 10. The major brain area containing HSV-1 DNA was the midbrain. Small amount of HSV-1 copy numbers were found in other regions ($P < .05$). In the peripheral nervous system, viral DNA was detected in the trigeminal ganglia from day 2 to day 4, but became undetectable after this time. We have previously described that in other organs (as liver, kidney, pancreas, spleen, bone marrow, or heart), no virus was detected (Burgos *et al*, 2002a, 2005).

Effect of viral dose

To evaluate the influence of the injected viral dose on colonization, experiments with doses ranging from 10^6 to 10^8 PFU were performed in wild-type mice (sacrificed at 10 dpi, when the HSV-1 DNA load in the brain had reached its highest). Figure 2 shows the HSV-1 DNA concentration detected was dependent on the viral dose. All the doses analyzed, however, produced a similar pattern of infection. Independent of the dose injected, the blood was the organ with the highest viral DNA concentration, followed by the nervous system (spinal cord, brain, and trigeminal ganglia). This confirms the anatomical and functional connection between viremia and the migration

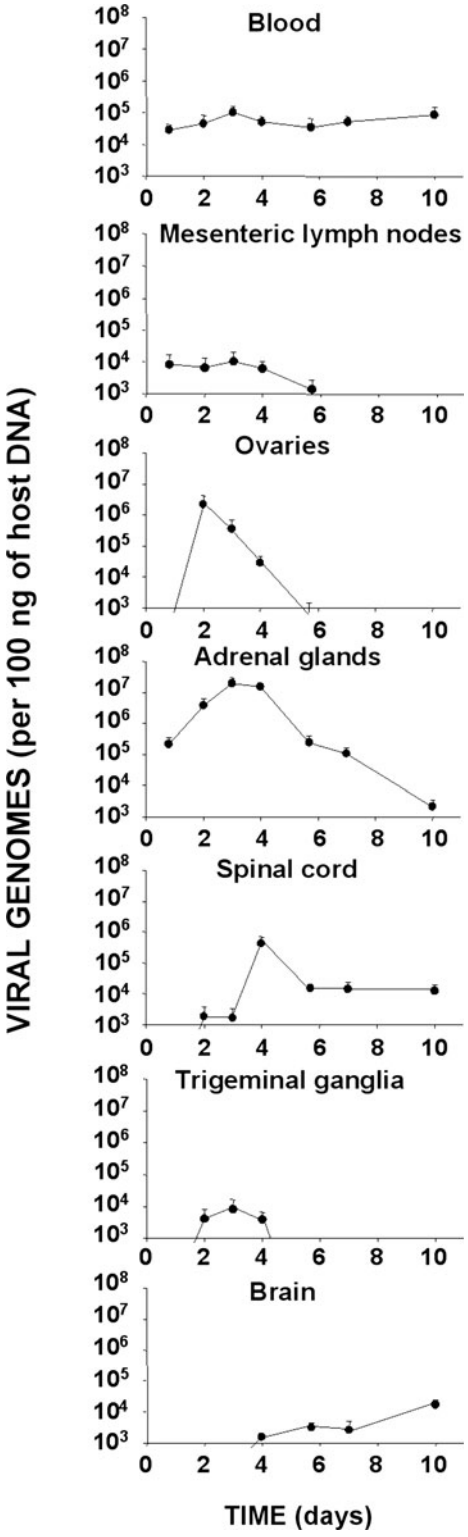

Figure 1 Time courses of HSV-1 infection in the analyzed organs. Thirty five, 14-week-old, wild-type mice were i.v. inoculated with a suspension of 10^6 PFU of HSV-1 (F strain), sacrificed, and dissected at several time points (from 0.8 to 10 days post infection [dpi]). Lines represent the viral copy numbers detected in each organ expressed on a logarithmic scale. Values are the mean ± SEM of the quantity of viral DNA (expressed as viral genomes and normalized with respect to the quantity of mouse genomes in 100 ng of host DNA).

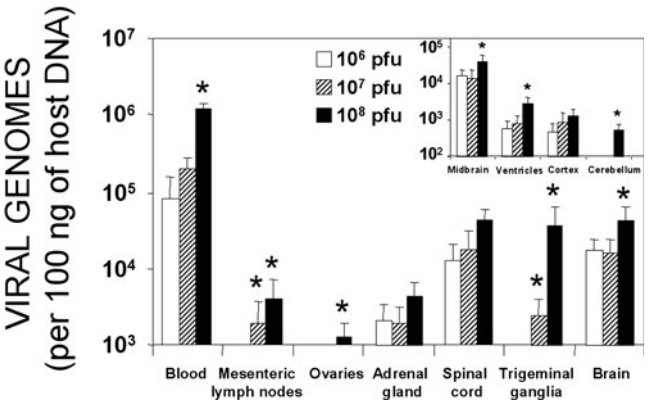

Figure 2 HSV-1 DNA concentrations in several organs with respect to the viral dose injected. Twenty-two, 14-week-old, wild-type mice were i.v. inoculated with HSV-1 (F strain) suspensions ranging from 10^6 to 10^8 PFU, sacrificed, and dissected at 10 dpi. The bar graph shows the viral copy numbers detected in each organ expressed on a logarithmic scale. Values are the mean ± SEM of the quantity of viral DNA (expressed as viral genomes and normalized with respect to the quantity of mouse genomes in 100 ng of host DNA). Inset: the areas of the brain analyzed in this study. Fisher's exact test was used to compare the viral DNA levels obtained with the different doses (always compared to a 10^6 PFU dose) ($*P < .05$).

of viruses to the central nervous system (CNS) (Burgos *et al*, 2002a). The right inset of Figure 2 shows the viral DNA concentrations in the four brain regions analyzed (the dose-dependent trend was confirmed for each). The midbrain had the highest viral DNA concentrations for every dose tested, followed by the ventricles, cortex, and cerebellum.

Influence of the ICP47-TAP interaction on viral invasiveness

Four experimental conditions were used to determine the influence of ICP47 protein on viral invasiveness when coupled to murine TAP (Figure 3): (i) HSV-1 F strain and normal mice, (ii) ΔICP47 virus and normal mice, (iii) HSV-1 F strain and TAP knockout mice, and (iv) ΔICP47 virus and TAP knockout mice. When normal mice were infected with ΔICP47, very low viral copy numbers were detected in every organ tested, except the blood. Interestingly, viral DNA levels in the bloodstream were constant, independent of the test condition. In contrast, normal mice infected with HSV-1 F strain showed the expected levels. This indicates that ICP47 is essential for the virus to be infective. No significant differences in viral load were observed between normal and TAP knockout mice when infected with HSV-1 F strain. However, when TAP knockout mice were challenged with ΔICP47 virus, the nervous system became infected. Interestingly, no significant differences were seen in the viral loads of the brain or trigeminal ganglia between TAP knockout mice infected with ΔICP47 and normal mice infected with the HSV-1 F strain. This indicates that the relationship between ICP47 and murine TAP is restricted to the nervous system.

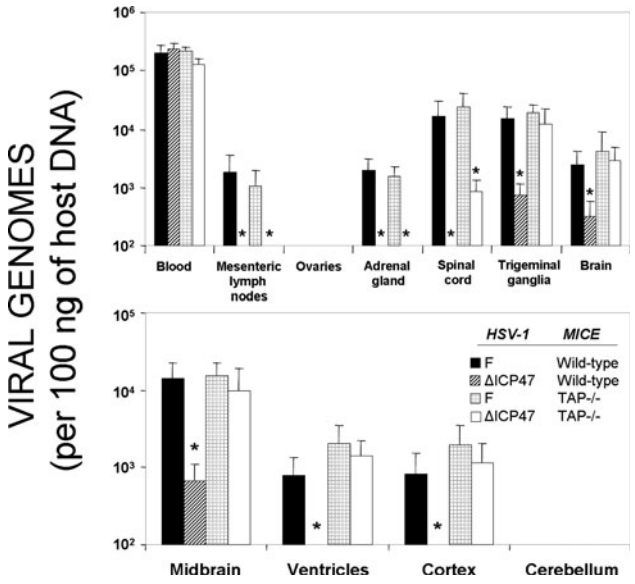

Figure 3 HSV-1 DNA concentrations with respect to the presence of viral ICP47 and/or murine TAP. Sixteen wild-type and 15 TAP-knockout mice (14 weeks old) were i.v. inoculated with a suspension of 10^7 PFU of HSV-1 (strain F or ΔICP47), sacrificed, and dissected at 10 dpi. The bar graph shows the viral copy numbers detected in each organ expressed on a logarithmic scale. Values are the mean ± SEM of the quantity of viral DNA (expressed as viral genomes and normalized with respect to the quantity of mouse genomes in 100 ng of host DNA). Fisher's exact test was used to compare the viral DNA levels among groups (comparison always performed against the condition involving F strain and wild-type mice [*black bars*]) (* $P < .05$).

When the encephalon was subdivided into different regions, similar trends were observed with ΔICP47 virus showing significantly reduced neuroinvasiveness in every region tested in the wild-type mice. Again, a recovery in the infective capacity of ΔICP47 was observed when TAP−/− mice were infected, indicating the specific interaction of TAP and ICP47 in neural cells. In contrast, the infectiveness of the HSV-1 F strain was the same in TAP knockout mice and wild-type mice.

TAP1 expression in mock-infected and infected mice

Western blotting was performed on lysates derived from the brains and adrenal glands of uninfected and infected mice using an affinity-purified polyclonal antibody against the C-terminal sequence of TAP1. A specific protein was detected with a molecular weight of around 71 KDa (the reporter molecular mass of TAP1) both in mock and infected mice, and in both organs (Figure 4, *top*). However, this band was not detected in organs from TAP knockout mice.

TAP1 was readily detected in the encephalons of infected animals, but only weakly detected in those of mock-infected animals, showing this protein to be strongly overexpressed in infected mice. Similar observations were made when the adrenal glands of infected and mock-infected animals were compared.

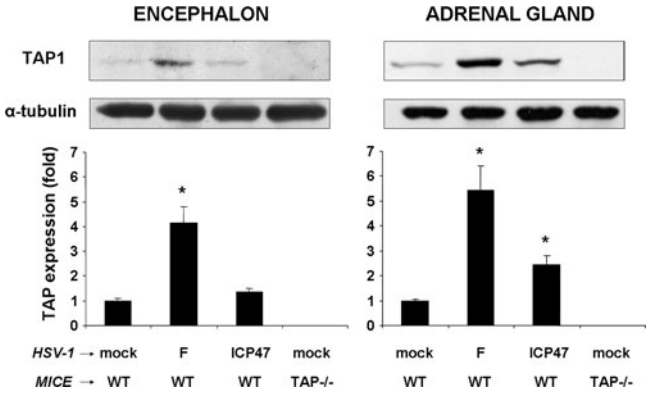

Figure 4 Influence of viral infection on TAP1 level in the brain and adrenal glands. Eleven wild-type [WT] and TAP-knockout [TAP−/−] mice (14 weeks old) were i.v. inoculated with a suspension of 10^7 PFU of HSV−1 (F strain [F] or ΔICP47) or with saline solution [mock], sacrificed, and dissected at 10 dpi. (*Top*) Representative Western blot showing a 71 Kda band corresponding to TAP1 expression in different pools of brain and adrenal gland samples, normalized with α-tubulin (55 KDa band). (*Bottom*) Quantification by densitometry of TAP1 expression (mean of at least three independent experiments). Bars indicate expression of TAP1 in infected (both types of virus) and mock-infected mice in each organ analyzed. Values are means ± SEM. Fisher's exact test was used to compare TAP1 levels among groups (comparison always performed against the result for uninfected wild-type mice) (* $P < .05$).

The densitometer data showed 4.1- and 5.4-fold increases in TAP1 levels as a consequence of infection of the brain and adrenal glands respectively (Figure 4, *bottom*). The results for individual animals were similar to the means of the pools to which they belonged. Thus, TAP1 overexpression appears to be a consequence of HSV-1 infection irrespective of the tissue analyzed; protein overexpression appears to occur only when infection of the organ has taken place.

Uninfected encephalons showed significantly lower baseline TAP1 levels than did uninfected adrenal glands (adrenal TAP1/brain TAP1 ratio > 100). This suggests that, given the low concentration of this protein in the brain, changes in TAP expression might be more important for regulating infection in the nervous system than in other areas.

ΔICP47 infection provoked a very limited, although significant, increase in TAP1 in the adrenal glands. No significant changes were observed, however, when the encephalon was infected with ΔICP47, indicating that a minimum threshold of infection is required to cause TAP1 overexpression. This is especially true of the brain where the baseline levels of TAP1 are low.

Discussion

The results show that ΔICP47 is less invasive than HSV-1 F strain in wild-type mice ($P < .05$), although ΔICP47 recovers its infectiveness in the absence of

TAP. This phenomenon, however, is restricted to the nervous system; no differences in infectiveness were seen in the peripheral organs in the presence or absence of TAP. The results also show that infection with the HSV-1 F strain provokes an important increase in TAP1 in infected organs. However, ΔICP47 virus cannot stimulate TAP1 overexpression even in the brain.

After intravenous (i.v.) inoculation with the HSV-1 F strain, viral genomes were immediately detectable in blood and later in the adrenal gland and ovary. The virus eventually reached the spinal cord and then migrated to the brain. The midbrain, the first site reached in acute infection, showed the highest levels of viral DNA. This work confirms our previous results obtained with intraperitoneally (i.p.) inoculated KOS strain viruses (Burgos *et al*, 2002a, 2003, 2005, 2006a, 2006b).

Hematogenous infection of HSV-1 has been described in human newborns (Arvin *et al*, 1982) and immunosuppressed individuals (Montgomerie *et al*, 1969), but although other routes of infection (oral, ocular, or genital) present a higher frequency of acquisition (Johnson, 1964), interest in the hematogenous route has grown in recent years. To that effect, differences in neuroinvasiveness should be attributable to the different inoculation route. To that effect, Goldsmith and coworkers (1998), using an ocular model of HSV-1 infection, investigated the ICP47 role in the neuroinvasiveness (but other routes of infection or the role of TAP was not analyzed in this report).

ICP47 is an HSV immediate-early protein that binds specifically to the MHC-encoded peptide transporter complex, thereby blocking the supply of peptide for the correct assembly and trafficking of MHC class I molecules (York *et al*, 1994). Consequently, antigen presentation is turned off and the infected cells are hidden from the immune system. Although to date ICP47 has been described to play a key role in the persistence of HSV infection, few studies have analyzed the involvement of this protein in viral virulence and/or invasiveness. Because the contribution of ICP47 to viral infection cannot be readily determined in humans, animal models are required, although the results they provide must be interpreted with caution. It is reasonable to assume that a viral protein that specifically inhibits $CD8^+$ T-cell function might not dramatically affect HSV-1 disease in the cornea or skin of the mouse, but this might not be the case in nervous tissue following hematogenous infection. The present results show that, compared to HSV-1 F strain, ΔICP47 is much less infective. The pattern of infection seen in normal mice after intravenous infection with ΔICP47 consistently showed ICP47 to be required for infection to occur beyond the bloodstream. Thus, the absence of ICP47 limits the capacity of the virus to colonize the neurons, and suggests it might be an exceptional target for antiviral drugs. Moreover, the HSV-1 F strain, and not the ΔICP47 mutant, managed to invade every organ tested, both in the wild-type and TAP knockout mice. This indicates that ICP47 plays an important role in the infection of all organs.

Interestingly, the present results also show that ΔICP47 can recover its neuroinvasiveness when TAP is absent. This recovery appears to be more powerful the closer to the brain. Indeed, while ΔICP47 DNA levels showed an upward trend in the spinal cord in TAP knockout mice compared to wild-type animals, in the brain they were completely recovered. This same phenomenon was seen in all brain regions analyzed. The trigeminal ganglia, the main reservoir of the virus in the peripheral nervous system (Steiner and Kennedy, 1995) (and, in fact, where the pattern of MHC class I expression is unknown), showed the same coupling to take place between ICP47 and TAP. This suggests that TAP plays a critical role in the infection of the nervous system. However, it remains unknown whether impaired TAP expression is the result of interference at the transcriptional level or the consequence of the inhibition of TAP function by viral proteins (Momburg and Hengel, 2002). Moreover, the rescue of the neuroinvasiveness of the ΔICP47 virus in the TAP knockout background, together with the molecular mechanisms of the ICP47-TAP interaction described in cellular models, discard the need to test a revertant virus for ICP47 in the context of the brain colonization.

The capacity of HSV-1 to infect different organs may depend on the baseline level of TAP1 expression. There is evidence that human cells differ in their sensitivity to ICP47, e.g., lymphocytes express much higher levels of TAP than fibroblasts (Tomazin *et al*, 1996). The results showed the adrenal glands to have a higher baseline TAP1 expression than the brain (>100-fold), suggesting TAP levels to be more critical to successful infection in organs with low levels of the protein. Tissues that produce lower levels of TAP may therefore be at greater risk of infection.

Comparisons of TAP1 levels in infected organs showed TAP1 overexpression to be a consequence of infection, indicating that TAP is regulated by HSV-1. More serious infections might therefore be anticipated in syndromes where TAP is missing. The present results showed a dramatic increase in TAP1 expression in the brain and adrenal glands.

Although TAP1 overexpression was clearly detected in mice infected with HSV-1 F strain, ΔICP47 infection of the brain induced TAP1 protein levels that were no different to those seen in the mock-infected mice, i.e., they remained very low. This was probably more due to the low infectivity of ΔICP47 than to the direct up-regulation of TAP. Therefore, TAP overexpression appears to be a general phenomenon caused by efficient infection, independent of the organ affected, and could therefore be a host response mechanism to infection. Organs that produce little TAP, such as the encephalon, would therefore be at greater risk of becoming infected. We recently

reported a TAP2 gene polymorphism to be associated with Alzheimer's disease (AD)—which is consistent with the idea that certain isoforms of TAP (Bullido *et al*, 2006) might facilitate the access of HSV-1 to the brain. The presence of HSV-1 in the brain has been suggested to increase the risk of developing AD (Itzhaki, 2004; Jamieson *et al*, 1992; Lin *et al*, 1996).

It has been described that murine TAP is less efficient than human TAP in translocating peptides with basic carboxy termini (Momburg *et al*, 1994; Rammensee *et al*, 1993; Schumacher *et al*, 1994). For example, ICP47 has a 100-fold greater affinity for the human TAP complex than its murine counterpart (Ahn *et al*, 1996). Assuming a comparable baseline level of antigen processing and presentation in the mouse and human nervous systems, it might be predicted that TAP would have a far more profound effect on HSV-1 neurovirulence in humans. Further, the results of the present work suggest that endogenous TAP might have a special role in preventing the infection of the human brain. Thus, the low inducible TAP levels of the nervous system might increase its susceptibility to HSV-1 infection.

In conclusion, the present results indicate that the absence of ICP47 inhibits HSV-1 infection of the peripheral organs independent of the participation of murine TAP. In the nervous system, however, TAP plays an important role in controlling infection. The importance of ICP47 in the process by which HSV-1 infects the brain suggests that this viral protein could be an excellent target for antiviral drugs. Further *in vivo* studies are needed to better understand the interaction between ICP47 and TAP.

Materials and methods

Animals and viruses

All experiments were performed in accordance with the guidelines of the 1986 European Community Animals Act (Scientific Procedures). All animals underwent a period of quarantine. Strict precautions were taken to prevent contamination during inoculation and dissection.

The experimental animals were 112 C57BL/6J female mice: 89 wild-type mice and 23 TAP knockout (TAP−/−) mice (B6.129S2-*Tap1*^{tm1Arp}/J) generated using the Tonegawa protocol (Van Kaer *et al*, 1992). All animals were supplied by the Jackson Laboratory (Bar Harbor, MA, USA). All were individually marked, housed in the same suite (in groups of five) under pathogen-free conditions, and used in experiments at 14 weeks of age.

HSV-1 was propagated and titrated by plaque assay in confluent monolayers of Vero cells (Burgos *et al*, 2002a). The HSV-1 F strain—wild-type (obtained from the American Type Culture Collection) and the ICP47-deficient mutant (ΔICP47) (kindly supplied by B. Roizman) (Mavromara-Nazos *et al*, 1986)—was used in all experiments.

Inoculation and dissection

Female mice were intravenously (i.v.) infected by injecting 100 μl suspensions of 10^6, 10^7, or 10^8 plaque forming units (PFU) of virus into the tail vein. All animals were monitored every day for symptoms. The mouse strain and the female gender were selected to facilitate the comparison of the results with published data (Burgos *et al*, 2002a, 2003, 2005). Females were also used because they show greater infectivity than males (Burgos *et al*, 2005). Mock-infected mice were used as controls.

Five or more animals from each experimental group (depending on availability) were sacrificed at each time point (between 18 h and 10 days post infection [dpi]) with CO_2-enriched air. The mesenteric lymph nodes, gonads, adrenal glands, spinal cord, trigeminal ganglia, brain and whole blood samples were removed and frozen at −70°C. For more detailed analyses, the brain samples were subdivided into four regions: the *midbrain* (including the midbrain and nearby structures such as the pons, the medulla, and the superior and inferior colliculus), the *ventricles* (including the third and lateral ventricles, the thalamus, the hypothalamus, the preoptic area, and the striatum), the *cerebral cortex* (including the cortex, the temporal, frontal, parietal and occipital lobes, the hippocampus, the corpus callosum, and the olfactory bulbs), and the *cerebellum*. For comparison among groups, infected animals (10^7 PFU) were culled at day 10. This time point was selected because it coincides with the highest viral DNA concentration in the brain.

HSV-1 DNA quantification in tissue homogenates

DNA from homogenized samples was extracted by conventional methods (High Pure PCR template preparation kit; catalog no. 1 796 828, Roche, Germany). The concentration of HSV-1 DNA in several organs was then determined by real-time quantitative PCR as previously described (Burgos *et al*, 2002b). An appropriate concentration range of purified HSV-1 DNA was used to optimize the standard curve, and the viral DNA concentration expressed in terms of viral copy numbers. Polymerase chain reaction (PCR) calibration was performed using the β-actin housekeeping gene (results expressed as nanograms of host DNA). Real-time PCR was performed using a LightCycler rapid thermal cycler (Roche Diagnostics, Lewes, UK) and a LightCycler FastStart DNA Master SYBR Green I kit (catalog no. 3 003 230, Roche, Germany). β-Actin primers (5′-AAC CCT AAG GCC AAC CGT GAA AAG ATG ACC-3′ and 5′-CCA GGG AGG AAG AGG ATG CGG C-3′) were used as a positive control for the reaction (379-bp PCR product). Specific primers were prepared for a sequence in the viral DNA thymidine kinase (TK) gene (5′-ATA CCG ACG ATC TGC GAC CT-3′ and 5′-TTA TTG CCG TCA TAG CGC GG-3′; 110 bp product). The reaction conditions were 95°C for 10 min, followed by 50 cycles at 95°C for 30 s, 55°C for 30 s (for

β-actin) or 60°C for 5 s (for TK), and 72°C for 40 s. Each experiment was performed in triplicate. Melting curve analyses, agarose and acrylamide gel electrophoresis, restriction analysis and nested-PCR confirmed the specificity of the products (Burgos *et al*, 2002b, 2006b).

Western blotting

Brains and adrenal glands from mock and infected mice (10^7 PFU) ($n = 10$) were homogenized in 400 μl phosphate-buffered saline (PBS) in a Mixer Mill Type MM 300 (Retsch, Hann, Germany). Fifty microliters of these homogenates were then lysed in an ice-water bath for 30 min in lysis buffer (300 mM NaCl, 50 mM Tris-HCl pH 7.6, 0.5% Triton X-100, protease inhibitor cocktail [Roche Diagnostics, Germany]). The lysates were centrifuged at 1870 $\times$ *g* for 15 min at 4°C, and the supernatants boiled with Sodium dodecyl sulfate–polyacrylamide gel electrophoresis (SDS-PAGE) sample buffer (250 mM Tris-HCl pH 6.8, 0.5 M dithiothreitol, 10% SDS, 0.5% bromophenol blue, 50% glycerol). Protein quantification was performed by the Bradford method (BioRad Protein Assay, Munich, Germany). Thirty-microgram samples were subjected to SDS-PAGE in 10% polyacrylamide gels (Laemmli, 1970) and transferred to nitrocellulose membranes (BioRad) (Towbin *et al*, 1979). The latter were blocked overnight at 4°C with PBS, 3% bovine serum albumin (BSA), 0.2% Tween 20 prior to incubation with the primary antibody. The anti-TAP1 antibody (M-18, Santa Cruz, US) was used at a dilution of 1/100 in PBS, 1% BSA, 0.05% Tween 20 for 90 min at room temperature. The blot was washed (3 $\times$ 10 min) in PBS, 0.05% Tween 20. Secondary antibodies (peroxidase-linked rabbit anti-goat Immunoglobulin G [IgG] [Sigma-Aldrich]) were applied in PBS (dilution 1/50,000), 1% BSA, 0.05% Tween 20 for 90 min at room temperature. As an internal control, α-tubulin levels were examined in the same blot using monoclonal anti-α-tubulin (Sigma) (Recuero *et al*, 2004). The blots were washed again (3 $\times$ 10 min) and bands visualized using the enhanced chemiluminiscence Western-blotting analysis system (Pharmacia Biotech).

Statistical analysis

Differences between the groups with respect to HSV-1 DNA concentration or TAP1 protein expression were examined using Fisher's exact test. Significance was set at $P < .05$.

References

Ahn K, Meyer TH, Uebel S, Sempe P, Djaballah H, Yang Y, Peterson PA, Fruh K, Tampe R (1996). Molecular mechanism and species specificity of TAP inhibition by herpes simplex virus ICP47. *EMBO J* **15:** 3247–3255.

Arvin AM, Yeager AS, Bruhn FW, Grossman M (1982). Neonatal herpes simplex infection in the absence of mucocutaneous lesions. *J Pediatr* **100:** 715–721.

Bullido MJ, Martinez-Garcia A, Artiga MJ, Aldudo J, Sastre I, Gil P, Coria F, Muñoz DG, Hachinski V, Frank A, Valdivieso F (2006). A TAP2 genotype associated with Alzheimer's disease in APOE4 carriers. *Neurobiol Aging* at press.

Burgos JS, Guzman-Sanchez F, Sastre I, Fillat C, Valdivieso F (2006a). Non-invasive bioluminescence imaging for monitoring herpes simplex virus type 1 hematogenous infection. *Microbes Infect* **8:** 1330–1338.

Burgos JS, Ramirez C, Guzman-Sanchez F, Alfaro JM, Sastre I, Valdivieso F (2006b). Hematogenous vertical transmission of herpes simplex virus type 1 in mice. *J Virol* **80:** 2823–2831.

Burgos JS, Ramirez C, Sastre I, Alfaro JM, Valdivieso F (2005). Herpes simplex virus type 1 infection via the bloodstream with apolipoprotein E dependence in the gonads is influenced by gender. *J Virol* **79:** 1605–1612.

Burgos JS, Ramirez C, Sastre I, Bullido MJ, Valdivieso F (2002a). Involvement of apolipoprotein E in the hematogenous route of herpes simplex virus type 1 to the central nervous system. *J Virol* **76:** 12394–12398.

Burgos JS, Ramirez C, Sastre I, Bullido MJ, Valdivieso F (2003). ApoE4 is more efficient than E3 in brain access by herpes simplex virus type 1. *Neuroreport* **14:** 1825–1827.

Burgos JS, Ramirez C, Tenorio R, Sastre I, Bullido MJ (2002b). Influence of reagents formulation on real-time PCR parameters. *Mol Cell Probes* **16:** 257–260.

Fruh K, Ahn K, Djaballah H, Sempe P, van Endert PM, Tampe R, Peterson PA, Yang Y (1995). A viral inhibitor of peptide transporters for antigen presentation. *Nature* **375:** 415–418.

Gadola SD, Moins-Teisserenc HT, Trowsdale J, Gross WL, Cerundolo V (2000). TAP deficiency syndrome. *Clin Exp Immunol* **121:** 173–178.

Galocha B, Hill A, Barnett BC, Dolan A, Raimondi A, Cook RF, Brunner J, McGeoch DJ, Ploegh HL (1997). The active site of ICP47, a herpes simplex virus-encoded inhibitor of the major histocompatibility complex (MHC)-encoded peptide transporter associated with antigen processing (TAP), maps to the NH_2-terminal 35 residues. *J Exp Med* **185:** 1565–1572.

Goldsmith K, Chen W, Johnson DC, Hendricks RL (1998). Infected cell protein (ICP)47 enhances herpes simplex virus neurovirulence by blocking the CD8+ T cell response. *J Exp Med* **187:** 341–348.

Hill A, Jugovic P, York I, Russ G, Bennink J, Yewdell J, Ploegh H, Johnson D (1995). Herpes simplex virus turns off the TAP to evade host immunity. *Nature* **375:** 411–415.

Hill A, Ploegh H (1995). Getting the inside out: the transporter associated with antigen processing (TAP) and the presentation of viral antigen. *Proc Natl Acad Sci U S A* **92:** 341–343.

Hill AB, Barnett BC, McMichael AJ, McGeoch DJ (1994). HLA class I molecules are not transported to the cell surface in cells infected with herpes simplex virus types 1 and 2. *J Immunol* **152:** 2736–2741.

Itzhaki R (2004). Herpes simplex virus type 1, apolipoprotein E and Alzheimer' disease. *Herpes* **11 (Suppl 2):** 77A–82A.

Jamieson GA, Maitland NJ, Wilcock GK, Yates CM, Itzhaki RF (1992). Herpes simplex virus type 1 DNA is present in specific regions of brain from aged people with and without senile dementia of the Alzheimer type. *J Pathol* **167:** 365–368.

Johnson RT (1964). The pathogenesis of herpes virus encephalitis. I. Virus pathways to the nervous system of suckling mice demonstrated by fluorescent antibody staining. *J Exp Med* **119:** 343–356.

Kern ER, Overall JC, Jr, Glasgow LA (1973). Herpesvirus hominis infection in newborn mice. I. An experimental model and therapy with iododeoxyuridine. *J Infect Dis* **128:** 290–299.

Laemmli UK (1970). Cleavage of structural proteins during the assembly of the head of bacteriophage T4. *Nature* **227:** 680–685.

Lascano EF, Berria MI (1980). Histological study of the progression of herpes simplex virus in mice. *Arch Virol* **64:** 67–79.

Lin WR, Shang D, Itzhaki RF (1996). Neurotropic viruses and Alzheimer disease. Interaction of herpes simplex type 1 virus and apolipoprotein E in the etiology of the disease. *Mol Chem Neuropathol* **28:** 135–141.

Mavromara-Nazos P, Ackermann M, Roizman B (1986). Construction and properties of a viable herpes simplex virus 1 recombinant lacking coding sequences of the alpha 47 gene. *J Virol* **60:** 807–812.

Momburg F, Hengel H (2002). Corking the bottleneck: the transporter associated with antigen processing as a target for immune subversion by viruses. *Curr Top Microbiol Immunol* **269:** 57–74.

Momburg F, Roelse J, Howard JC, Butcher GW, Hammerling GJ, Neefjes JJ (1994). Selectivity of MHC-encoded peptide transporters from human, mouse and rat. *Nature* **367:** 648–651.

Montgomerie JZ, Becroft DM, Croxson MC, Doak PB, North JD (1969). Herpes-simplex-virus infection after renal transplantation. *Lancet* **2:** 867–871.

Orr MT, Edelmann KH, Vieira J, Corey L, Raulet DH, Wilson CB (2005). Inhibition of MHC class I is a virulence factor in herpes simplex virus infection of mice. *PLoS Pathogens* **1:** 62–71.

Rammensee HG, Falk K, Rotzschke O (1993). Peptides naturally presented by MHC class I molecules. *Annu Rev Immunol* **11:** 213–244.

Recuero M, Serrano E, Bullido MJ, Valdivieso F (2004). Abeta production as consequence of cellular death of a human neuroblastoma overexpressing APP. *FEBS Lett* **570:** 114–118.

Schumacher TN, Kantesaria DV, Heemels MT, Ashton-Rickardt PG, Shepherd JC, Fruh K, Yang Y, Peterson PA, Tonegawa S, Ploegh HL (1994). Peptide length and sequence specificity of the mouse TAP1/TAP2 translocator. *J Exp Med* **179:** 533–540.

Spies T, Bresnahan M, Bahram S, Arnold D, Blanck G, Mellins E, Pious D, DeMars R (1990). A gene in the human major histocompatibility complex class II region controlling the class I antigen presentation pathway. *Nature* **348:** 744–747.

Steiner I, Kennedy PG (1995). Herpes simplex virus latent infection in the nervous system. *J NeuroVirol* **1:** 19–29.

Tomazin R, Hill AB, Jugovic P, York I, van Endert P, Ploegh HL, Andrews DW, Johnson DC (1996). Stable binding of the herpes simplex virus ICP47 protein to the peptide binding site of TAP. *EMBO J* **15:** 3256–3266.

Towbin H, Staehelin T, Gordon J (1979). Electrophoretic transfer of proteins from polyacrylamide gels to nitrocellulose sheets: procedure and some applications. *Proc Natl Acad Sci U S A* **76:** 4350–4354.

Townsend A, Bodmer H (1989). Antigen recognition by class I-restricted T lymphocytes. *Annu Rev Immunol* **7:** 601–624.

Van Kaer L, Ashton-Rickardt PG, Ploegh HL, Tonegawa S (1992). TAP1 mutant mice are deficient in antigen presentation, surface class I molecules, and CD4-8+ T cells. *Cell* **71:** 1205–1214.

York IA, Roop C, Andrews DW, Riddell SR, Graham FL, Johnson DC (1994). A cytosolic herpes simplex virus protein inhibits antigen presentation to CD8+ T lymphocytes. *Cell* **77:** 525–535.